ACS Medicinal Chemistry Letters

Letter

pubs.acs.org/acsmedchemlett

From in Silico Discovery to Intracellular Activity: Targeting JNK–Protein Interactions with Small Molecules

Tamer S. Kaoud,[†,‡,+] Chunli Yan,[#,+] Shreya Mitra,[▽] Chun-Chia Tseng,[†] Jiney Jose,[†] Juliana M. Taliaferro,[†,‡] Maidina Tuohetahuntila,[†] Ashwini Devkota,[†,⊥] Rachel Sammons,[§,#] Jihyun Park,[†,∥] Heekwang Park,[○] Yue Shi,[§,#] Jiyong Hong,[○] Pengyu Ren,*[,§,#] and Kevin N. Dalby*[,†,‡,§,∥,⊥,¶]

[†]Division of Medicinal Chemistry, Graduate Programs in [‡]Pharmacy, [§]Biomedical Engineering, and [∥]Cell and Molecular Biology, [⊥]Texas Institute for Drug and Diagnostic Development, and [#]Department of Biomedical Engineering, University of Texas at Austin, Austin, Texas 78712, United States

[▽]The University of Texas MD Anderson Cancer Center, Houston, Texas 77030, United States

[○]Department of Chemistry, Duke University, Durham, North Carolina 27708, United States

Supporting Information

ABSTRACT: The JNK–JIP1 interaction represents an attractive target for the selective inhibition of JNK-mediated signaling. We report a virtual screening (VS) workflow, based on a combination of three-dimensional shape and electrostatic similarity, to discover novel scaffolds for the development of non-ATP competitive inhibitors of JNK targeting the JNK–JIP interaction. Of 352 (0.13%) compounds selected from the NCI Diversity Set, more than 22% registered as hits in a biochemical kinase assay. Several compounds discovered to inhibit JNK activity under standard kinase assay conditions also impeded JNK activity in HEK293 cells. These studies led to the discovery that the lignan (−)-zuonin A inhibits JNK–protein interactions with a selectivity of 100-fold over ERK2 and p38 MAPKα. These results demonstrate the utility of a virtual screening protocol to identify novel scaffolds for highly selective, cell-permeable inhibitors of JNK–protein interactions.

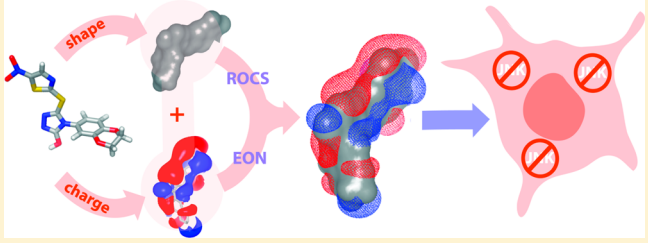

KEYWORDS: *virtual screening, JNK, non-ATP competitive inhibitor, JNK–JIP interaction, molecular docking and dynamics*

c-Jun N-terminal kinases (JNKs) belong to the mitogen-activated protein kinase (MAPK) family and are encoded by three genes (*Jnk1*, *Jnk2*, and *Jnk3*), which produce at least 10 different spliceforms. JNK1 and JNK2 show a broad tissue distribution, whereas JNK3 expression is more restrictive.[1] JNK1−3 are activated by extracellular stimuli, such as stress or cytokines, which leads to the phosphorylation of several cellular substrates implicated in cell survival and proliferation.[2,3]

The JNK signaling pathway is associated with the pathogenesis of several diseases, including diabetes, cancer, and neurological diseases.[4,5] Most drug discovery efforts have focused on the development of ATP-competitive inhibitors of JNK,[6] which presents challenges due to the high level of homology in the ATP-binding site among protein kinases.[7]

An alternative strategy to develop a specific JNK inhibitor is to target a substrate recruitment site. Inhibitors that target the protein–protein interaction sites of MAPK kinases are expected to exhibit pharmacological profiles that are quite distinct from those that bind within the active site. Although the development of small molecules targeting protein–protein interactions represents a challenging area, progress has been made with a variety of approaches.[7] Scaffolding proteins, such as the JNK interacting proteins (JIP 1−4)[8] and arrestin,[9] are known to bind JNK to enhance its activation in vivo. Several non-ATP-competitive inhibitors of JNK target the JNK–JIP interaction. For example, JIP-based peptide inhibitors that correspond to the D-site of JIP1 bind the D-recruitment site (DRS) of JNK and act as specific inhibitors of JNK–ligand interactions.[10] Recently, we engineered potent (IC_{50} ~90 nM) JIP-based peptide inhibitors with demonstrated specificity for the JNK2 isoform.[11,12] In 2008, Stebbins et al. identified the thiadiazole BI-78D3 (Figure 1A) as a small molecule targeting the JNK–JIP interaction.[13] BI-78D3 was identified as a non-ATP competitive inhibitor of JNK. Several analogues of BI-78D3 with improved plasma stability have been reported.[14−16] There also have been efforts to discover different scaffolds that act as non-ATP inhibitors of JNK.[17,18]

In this work, we used ligand-based virtual screening (VS) to discover JNK-selective inhibitors that do not compete with ATP. The starting point for this virtual screen was BI-78D3 (Figure 1A). Ligand-based VS with BI-78D3 as the query molecule was applied to search the National Cancer Institute

Received: May 27, 2012
Accepted: August 6, 2012
Published: August 6, 2012

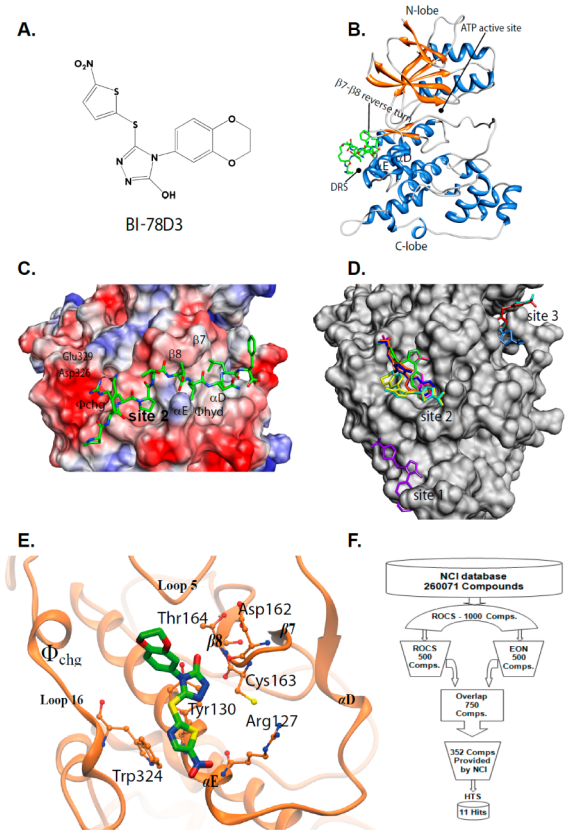

Figure 1. Ligand binding to JNK. (A) Chemical structure of BI-78D3. (B) Cartoon representation of JNK1 bound to pepJIP1 (amino acids 154−163: PKRPTTLNLF) (PDB ID: 1UKH).[10] (C) Surface representation of JNK1 bound to pepJIP1. (D) Molecular docking of BI-78D3 to JNK1. (E) Determination of the bioactive conformation for the query ligand BI-78D3 in complex with JNK1 using molecular dynamics. (F) Schematic representation of the virtual screening approaches adopted.

(NCI) Diversity Set[19] for selective inhibitors. The evaluation of selected compounds not only resulted in new scaffolds for the development of potential therapeutic agents that target the JNK−JIP interaction but also yielded the discovery that the lignan (−)-zuonin A inhibits JNK−protein interactions with a selectivity of 100-fold over ERK2 and p38 MAPKα.

BI-78D3 (Figure 1A) is known to displace pepJIP1 from JNK.[13] To gain insight into its potential bioactive conformations when bound to JNK1, we constructed a model of the protein−ligand complex using coordinates from the X-ray crystal structure of the JNK1·pepJIP1 complex[10] (Figure 1B,C), where pepJIP1 binds the DRS of JNK. We searched the surface of JNK1, centering on the DRS to construct a model for BI-78D3 bound to JNK1 using molecular docking. Three possible docking sites were identified (Figure 1D), including five potential poses (binding structures) at site 2, which is situated in between a negatively charged surface, Φ_{chg}, and a hydrophobic pocket, Φ_{hyd}, and further defined by β8, αE, loop 16, and αD (Figure 1E). The poses at site 2 were used as starting structures for further molecular dynamics (MD) simulations to determine the dynamically stable protein−ligand binding modes. These were then further interrogated by MM-PBSA [molecular mechanics/Poisson−Boltzmann (PB) solvent-accessible surface area methodology][20] to estimate their relative binding free energy. The estimated binding free energy ΔG_b of pose 5 was slightly more favored (Table S1 in the Supporting Information). Interestingly, after 3 ns of MD simulation, pose 5 reoriented to place the nitro group of BI-78D3 in the proximity of Glu-126 and Arg-127 (αE) (Figure 1E). Accordingly, the ligand conformer in this new pose was used as the bioactive conformation of BI-78D3 with which to carry out the virtual screen. It should be noted that Stebbins et al.[13] proposed an alternative binding mode with the benzodioxan moiety of BI-78D3 occupying the hydrophobic (Φ_{hyd}) region that corresponds to the highly conserved leucines of pepJIP1 (Figure 1C). This binding mode was not identified in our studies.

A schematic summary of the overall VS procedure utilized in this study is presented in Figure 1F. The library used in the ligand-based VS is the NCI Diversity Set, which contains 260071 compounds.[19] Each compound was expanded into a set of 20 three-dimensional conformations using Omega 2.3.2 of OpenEye software. The three-dimensional shape comparison between BI-78D3 and the molecules in the NCI Diversity Set was performed using ROCS 2.3.1. The top 1000 ranked compounds from the shape-based screen were then assessed for similarity to BI-78D3 using EON 2.0.1, which calculates an Electrostatic Tanimoto (ET) score, which is a measure of the electrostatic similarity between two small molecules.[21] A total of 750 compounds, representing the merging of the top 500 hits from the two screens, were subsequently selected for further biochemical screening using in vitro kinase assays (Table S2 in the Supporting Information).

Three hundred and fifty-two of the top 750 compounds were available from NCI. An enrichment experiment was performed to compare these compounds to 350 selected randomly from the same library. The % inhibition of both the in silico VS-selected and the randomly selected compounds (at 10 μM concentrations) toward JNK1 and Trpm7 (an atypical kinase) was determined using an in vitro kinase assay. While 80 of 350 compounds from the in silico analysis were identified as hits when screened at 10 μM against JNK1 (greater than 25% inhibition above a DMSO control), none of the randomly selected (JNK1 control) compounds inhibited JNK1 by more than 20% (Figure 2A). Trpm7, which has little sequence similarity to JNK,[22] exhibited limited inhibition when treated with either the VS-selected compounds or the random set (Figure 2A). Surprisingly, when assayed against substrates that target the DRS, the MAP kinases ERK2 and p38MAPKα showed broadly similar results to Trpm7 and eEF-2K (Figure 2B). Together, these results validate the VS protocol as a useful tool for the identification of inhibitors that target JNK1.

The VS strategy that we followed in this work is predicted to discover inhibitors that compete with JIP and c-Jun at the DRS of JNK. We decided to examine several promising hits (compounds **1**−**11**) in more detail (Figure 3A) and prepared authentic samples of both enantiomers of compound **2**, $\mathbf{2}^{(-)}$, and $\mathbf{2}^{(+)}$.[a] As would be expected, compounds **1**−**11** exhibit structural features similar to those found in BI-78D3, including either a benzo[*d*][1,3]dioxole moiety (compounds, **1**, **2**, **5**, **6**, and **8**), an aromatic ring containing an electronegative substituent (compounds **3**, **4**, **7**, **10**, and **11**) or a nitro group (compounds **7**, and **9**). Figure 3B,C shows the structural overlaps and electrostatic distribution, respectively, of several of the hits identified in the screen.

We performed dose−response curves on the HPLC-purified compounds, examining their ability to inhibit c-Jun phosphorylation by JNK2 in an in vitro kinase assay (Table 1). The inhibition profile for JNK1 and JNK2 were similar (Figure 2B),

dx.doi.org/10.1021/ml300129b | ACS Med. Chem. Lett. 2012, 3, 721−725

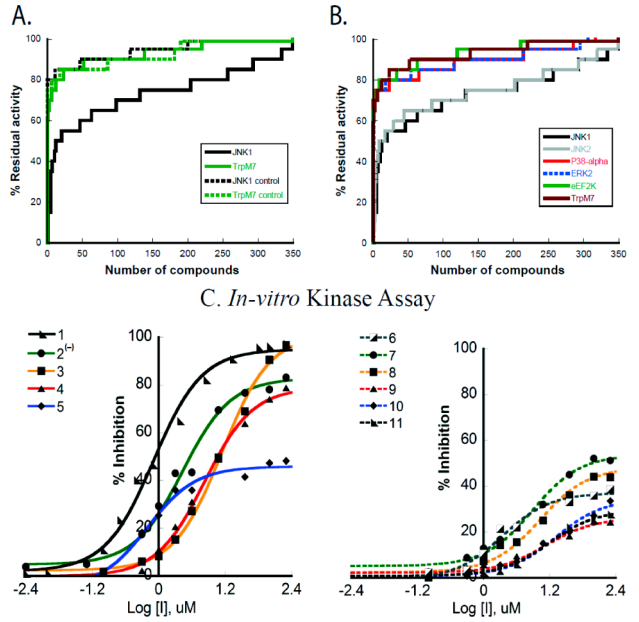

Figure 2. Assessing the selectivity of the virtual screen. (A) Comparing the activity of VS-selected (solid line) and randomly selected (dashed line) compounds against JNK1 and TrpM7. (B) Comparing the activity of VS-selected compounds against indicated kinases. (C) Inhibition of JNK2 by compounds **1**−**11**.

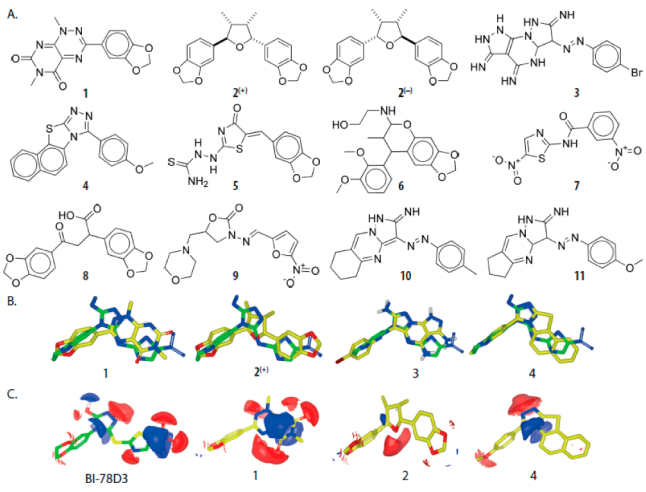

Figure 3. Top hits identified following biochemical screening. (A) Chemical structures of compounds **1**−**11**. (B) Overlay of indicated compounds (yellow carbons) and BI-78D3 (green carbons). (C) Three-dimensional chemical structures of indicated compounds and BI-78D8 with electrostatic surfaces coded by color (red for negative and blue for positive, MMFF94).

enabling us to use either JNK1 or JNK2 in the subsequent biochemical characterization of the compounds. As an additional biochemical screen, we developed a FITC-JIP peptide displacement assay to estimate the ability of compounds to displace JIP from JNK (Table 1). By using these two screens, compounds were assessed for their ability to inhibit the binding of two different D-site sequences to JNK.

IC_{50} values for the inhibition of JNK or the displacement of JIP by the hits ranged from 0.7 to 22 μM and from 2.2 to 41 μM, respectively (Table 1). The maximal inhibition of JNK1 in the kinase assay at saturating inhibitor ranged from 30 to 100%, and the maximal displacement of JIP in the binding assay

Table 1. Biochemical Analysis of Compounds 1−11[f]

no.	JNK2[a]	JNK2[b]	p38MAPKα[a]	ERK2[a]
1	0.7 ± 0.1[c] (100%)	ND[d]	0.5 ± 0.04[c] (50%)	1 ± 0.1[c] (50%)
$2^{(+)}$	2.5 ± 0.2 (15%)	ND	ND	ND
$2^{(-)}$	2.5 ± 0.2 (80%)	2.2 ± 0.4 (82%)	252 ± 22 (50%)	295 ± 34 (50%)
3	14 ± 1.3 (100%)	58 ± 6 (100%)	60 ± 10 (57%)	4.6 ± 0.1 (100)
4	21.5 ± 0.9 (80%)	41 ± 6.9 (90%)	2.3 ± 0.2 (24%)	7.5 ± 2 (47%)
5	0.63 ± 0.1 (50%)	1.7 ± 0.16 (50%)	NS[e]	NS
6	2.2 ± 0.16 (40%)	2.2 ± 0.18 (66%)	NS	NS
7	7.7 ± 1 (53%)	NS	NS	NS
8	10.7 ± 2 (48%)	43 ± 6 (50%)	197 ± 29 (25%)	57 ± 0.6 (45%)
9	13.5 ± 0.7 (20%)	NS	NS	NS
10	20 ± 2.2 (35%)	14.5 ± 1.3 (40%)	NS	NS
11	15.5 ± 3 (30%)	7.8 ± 1 (25%)	NS	NS

[a]Kinetic assay. [b]Displacement assay. [c]Determined in the presence of 100 units/mL catalase. [d]Not determined. [e]Not significant. [f]Values in the table represent IC_{50} (μM) and % inhibition at saturation. Dose−response curves for data conforming to inhibition were fitted to

$$V_0 = V' - \left(V' \frac{i}{i + IC_{50}}\right) + V_{00}$$

where V_0 is the observed rate, i is the concentration of inhibitor I, V' is the observed rate in the absence of inhibitor, V_∞ is the observed rate constant at saturating inhibitor, I; and IC_{50} is the concentration that leads to half the maximal change in V_0.

ranged from 25 to 100%. In general, the two assays correlate quite well. However, some compounds appeared to perform slightly better in one assay as compared to the other, which is not surprising given that the assays utilize different D-sites and experimental conditions. Compound **1** is the highest ranked compound by EON due to its electrostatic similarity to BI-78D3. It fully (100%) inhibits JNK2 at saturating concentrations exhibiting an IC_{50} value of 0.7 ± 0.1 μM (Figure 2C). As we expected it to be a redox cycling compound (RCC), due to the presence of a pyrimidotriazinedione cluster, it was assessed in the presence of 100 U/mL of catalase. However, catalase had no effect on its activity (Supporting Information).[23] Unfortunately, its fluorescence spectrum precluded an assessment using the displacement assay. As predicted by the virtual screen, $\mathbf{2}^{(+)}$ [(+)-zuonin A[a]] binds JNK1, displaying an IC_{50} of 2.6 ± 0.2 μM; however, it exhibits only 15% inhibition at saturation (Table 1). In contrast, its enantiomer $\mathbf{2}^{(-)}$, (−)-zuonin A, exhibits a more pronounced 80% inhibition at saturation in both assays (Figures 2C and S1 in the Supporting Information), with a similar IC_{50}. These data suggest that upon binding, $\mathbf{2}^{(-)}$ blocks the binding of the D-sites to JNK more effectively than $\mathbf{2}^{(+)}$. At saturation, compound **3** exhibits 100% inhibition in both assays, although it is 3-fold more effective in the kinase assay (IC_{50} of 14 ± 1.3 μM) as compared to the displacement assay (IC_{50} of 58 ± 6 μM) (Figure S1 in the Supporting Information). Compound **4** performs equally in both assays (IC_{50} of 21 and 41 μM, respectively, ∼80% max). Compounds **5**, **6**, **8**, and **10** exhibit maximal inhibitions of less than 50% in both assays. Compounds **7** and **9** inhibit c-Jun

dx.doi.org/10.1021/ml300129b | ACS Med. Chem. Lett. 2012, 3, 721−725

phosphorylation but do not displace labeled JIP peptide from JNK2. The potency of compound **11** was significantly diminished by 0.01% Triton X-100 (Figure S2 in the Supporting Information), suggesting that its inhibition may be due to nonspecific binding or aggregation (Supporting Information).

To assess the nature of their interactions with JNK, we docked compounds **1**, **2**$^{(-)}$, **3**, and **4** onto the DRS of JNK1 (Figure S3 in the Supporting Information). The results of this analysis support the notion that all four compounds bind site 2. A MD analysis further suggests that the presence of a planar ring in proximity to the two aromatic rings of Tyr-130 and Trp-324 forms potentially favorable $\pi-\pi$ stacking interactions; however, it is clear that the orientations of the ring are predicted to vary significantly, suggesting that some compounds may form stronger interactions at this locus than others (Figures 1E and S3 in the Supporting Information). Differences in the binding modes for each compound could account for the variability in the maximal inhibition achieved at saturation (Figure S3 in the Supporting Information). This is an important consideration for the future development of analogues.

To profile the selectivity of the hits toward JNK, the IC_{50} of each compound was determined against ERK2 and p38MAPKα (Figure S4 in the Supporting Information and Table 1). Several compounds exhibited selectivity for JNK. Most notably, **2**$^{(-)}$ exhibits 100-fold selectivity for JNK2 over both ERK2 and p38MAPKα. Several other compounds **5**−**7**, **9**, and **10**, while less potent inhibitors of JNK, were also selective and in fact exhibited no significant inhibition of ERK2 or p38MAPKα. Compound **1** exhibited little selectivity between the MAPKs, while compounds **3** and **8** inhibited both JNK and ERK2, and compound **4** preferred ERK2 and p38. The selectivity profile of these compounds strongly demonstrates the ability of the VS protocol to identify molecules that target specific sites in JNK with acceptable selectivity.

Compounds such as **2**$^{(-)}$ have the potential to inhibit JNK signaling by compromising protein interactions with the DRS. The ability of the hits to inhibit JNK in HEK293 cells was therefore examined. The ability of each compound to inhibit the phosphorylation of JNK and c-Jun (a substrate of the JNKs[24]) was tested following stimulation of JNK by anisomycin[11] and visualized through Western blot analysis (Figures 4 and S5 in the Supporting Information). As expected, several compounds showed inhibition of JNK and c-Jun phosphorylation in HEK293 cells (e.g., **1**, **2**$^{(-)}$, and **6**).

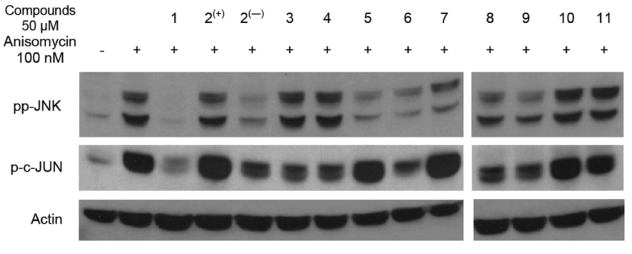

Figure 4. Cellular activity. (A) HEK293 cells were treated with DMSO or 50 μM indicated compound for 16 h and then stimulated with anisomycin (50−100 nM) for 5−10 min, before lysing the cells and analyzing JNK and c-Jun phosphorylation by Western blotting (one of three representative experiments shown; see Figure S5 in the Supporting Information).[11]

In conclusion, the NCI Diversity Set, consisting of approximately 260000 compounds, was virtually screened against the protein-binding site of JNK. A total of 11 small molecules were identified as potential inhibitors of JNK−JIP binding. (−)-Zuonin A showed marked selectivity for JNK over other MAPKs. Several of the inhibitors described here represent starting points for the development of potent and selective small molecules capable of compromising the binding of proteins to the DRS of JNK.

■ ASSOCIATED CONTENT

Ⓢ Supporting Information

Calculated binding free energies (kcal mol^{-1}) of BI-78D3 in complex with JNK1, NCI IDs of the compounds, ROCS and EON scores of the compounds, further characterization of the 11 hits, and detailed computational and experimental methods. This material is available free of charge via the Internet at http://pubs.acs.org.

■ AUTHOR INFORMATION

Corresponding Author

*E-mail: pren@mail.utexas.edu (P.R.) or kinases@me.com (K.N.D.).

Present Address

¶107 West Dean Keaton, BME, The University of Texas at Austin, Austin, Texas 78712, United States.

Author Contributions

⁺These authors contributed equally.

Funding

This research was supported in part by the grants from the Welch Foundation (F-1390), CPRIT (RP110539 and RP101501), and NIH (R01GM059802 and R01GM079686). Support from the Texas Advanced Computing Center (TACC) and TeraGrid (MCB100057) and The A. D. Hutchinson Student Endowment Fellowship (to T.S.K.) are acknowledged.

Notes

The authors declare no competing financial interest.

■ ACKNOWLEDGMENTS

We thank Dr. Philip LoGrasso for providing JNK plasmids and Dr. Eric V. Anslyn for providing laboratory space to J.J. Dr. Angel Syrett prepared the TOC figure.

■ ABBREVIATIONS

JNK, c-Jun N-terminal kinases; MAPK, mitogen-activated protein kinase; DRS, D-recruitment site; NCI, National Cancer Institute; VS, virtual screening; MD, molecular dynamics; DELFIA, dissociation-enhanced lanthanide fluorescent immunoassay; Trpm7, the kinase domain of human Trpm7 channel kinase, containing the last 462 amino acids (1403−1864) of Trpm7/ChaK1 (GenBank accession number AF346629); eEF2K, full length eukaryotic elongation factor 2 kinase

■ ADDITIONAL NOTE

[a]We report elsewhere (Kaoud, T. S.; et al. Submitted for publication) that 2$^{(+)}$, 5,5′-(2*R*,3*R*,4*S*,5*R*)-3,4-dimethyltetrahydrofuran-2,5-diyl)bis(benzo[*d*][1,3]dioxole) corresponds to the natural product (+)-zuonin A, while 2$^{(-)}$, 5,5′-((2*S*,3*R*,4*S*,5*S*)-3,4-dimethyltetrahydrofuran-2,5-diyl)bis(benzo[*d*][1,3]-dioxole), corresponds to (−)-zuonin A.

REFERENCES

(1) Barr, R. K.; Bogoyevitch, M. A. The c-Jun N-terminal protein kinase family of mitogen-activated protein kinases (JNK MAPKs). *Int. J. Biochem. Cell B* **2001**, *33* (11), 1047−1063.

(2) Kyriakis, J. M.; Avruch, J. Mammalian mitogen-activated protein kinase signal transduction pathways activated by stress and inflammation. *Physiol. Rev.* **2001**, *81* (2), 807−869.

(3) Pearson, G.; Robinson, F.; Gibson, T. B.; Xu, B. E.; Karandikar, M.; Berman, K.; Cobb, M. H. Mitogen-activated protein (MAP) kinase pathways: Regulation and physiological functions. *Endocr. Rev.* **2001**, *22* (2), 153−183.

(4) Manning, A. M.; Davis, R. J. Targeting JNK for therapeutic benefit: From JuNK to gold? *Nat. Rev. Drug Discovery* **2003**, *2* (7), 554−565.

(5) Bogoyevitch, M. A. Therapeutic promise of JNK ATP-noncompetitive inhibitors. *Trends Mol. Med.* **2005**, *11* (5), 232−239.

(6) Siddiqui, M. A.; Reddy, P. A. Small molecule JNK (c-Jun N-terminal kinase) inhibitors. *J. Med. Chem.* **2010**, *53* (8), 3005−3012.

(7) Schnieders, M. J.; Kaoud, T. S.; Yan, C.; Dalby, K. N.; Ren, P. Computational Insights for the Discovery of Non-ATP Competitive Inhibitors of MAP Kinases. *Curr. Pharm. Des.* **2012**, *18*, 1173−1185.

(8) Yasuda, J.; Whitmarsh, A. J.; Cavanagh, J.; Sharma, M.; Davis, R. J. The JIP group of mitogen-activated protein kinase scaffold proteins. *Mol. Cell. Biol.* **1999**, *19* (10), 7245−7254.

(9) Zhan, X.; Kaoud, T. S.; Dalby, K. N.; Gurevich, V. V. Nonvisual arrestins function as simple scaffolds assembling the MKK4-JNK3alpha2 signaling complex. *Biochemistry* **2011**, *50* (48), 10520−10529.

(10) Heo, J. S.; Kim, S. K.; Seo, C. I.; Kim, Y. K.; Sung, B. J.; Lee, H. S.; Lee, J. I.; Park, S. Y.; Kim, J. H.; Hwang, K. Y.; Hyun, Y. L.; Jeon, Y. H.; Ro, S.; Cho, J. M.; Lee, T. G.; Yang, C. H. Structural basis for the selective inhibition of JNK1 by the scaffolding protein JIP1 and SP600125. *EMBO J.* **2004**, *23* (11), 2185−2195.

(11) Kaoud, T. S.; Mitra, S.; Lee, S.; Taliaferro, J.; Cantrell, M.; Linse, K. D.; Van Den Berg, C. L.; Dalby, K. N. Development of JNK2-selective peptide inhibitors that inhibit breast cancer cell migration. *ACS Chem. Biol.* **2011**, *6* (6), 658−666.

(12) Mitra, S.; Lee, J. S.; Cantrell, M.; Van den Berg, C. L. c-Jun N-terminal kinase 2 (JNK2) enhances cell migration through epidermal growth factor substrate 8 (EPS8). *J. Biol. Chem.* **2011**, *286* (17), 15287−15297.

(13) Stebbins, J. L.; De, S. K.; Machleidt, T.; Becattini, B.; Vazquez, J.; Kuntzen, C.; Chen, L. H.; Cellitti, J. F.; Riel-Mehan, M.; Emdadi, A.; Solinas, G.; Karin, M.; Pellecchia, M. Identification of a new JNK inhibitor targeting the JNK-JIP interaction site. *Proc. Natl. Acad. Sci. U.S.A.* **2008**, *105* (43), 16809−16813.

(14) De, S. K.; Chen, L. H.; Stebbins, J. L.; Machleidt, T.; Riel-Mehan, M.; Dahl, R.; Chen, V.; Yuan, H.; Barile, E.; Emdadi, A.; Murphy, R.; Pellecchia, M. Discovery of 2-(5-nitrothiazol-2-ylthio)-benzo[d]thiazoles as novel c-Jun N-terminal kinase inhibitors. *Bioorg. Med. Chem.* **2009**, *17* (7), 2712−2717.

(15) De, S. K.; Stebbins, J. L.; Chen, L. H.; Riel-Mehan, M.; Machleidt, T.; Dahl, R.; Yuan, H.; Emdadi, A.; Barile, E.; Chen, V.; Murphy, R.; Pellecchia, M. Design, synthesis, and structure-activity relationship of substrate competitive, selective, and in vivo active triazole and thiadiazole inhibitors of the c-Jun N-terminal kinase. *J. Med. Chem.* **2009**, *52* (7), 1943−1952.

(16) De, S. K.; Chen, V.; Stebbins, J. L.; Chen, L. H.; Cellitti, J. F.; Machleidt, T.; Barile, E.; Riel-Mehan, M.; Dahl, R.; Yang, L.; Emdadi, A.; Murphy, R.; Pellecchia, M. Synthesis and optimization of thiadiazole derivatives as a novel class of substrate competitive c-Jun N-terminal kinase inhibitors. *Bioorg. Med. Chem.* **2010**, *18* (2), 590−596.

(17) Chen, T.; Kablaoui, N.; Little, J.; Timofeevski, S.; Tschantz, W. R.; Chen, P.; Feng, J.; Charlton, M.; Stanton, R.; Bauer, P. Identification of small-molecule inhibitors of the JIP-JNK interaction. *Biochem. J.* **2009**, *420* (2), 283−294.

(18) Comess, K. M.; Sun, C.; Abad-Zapatero, C.; Goedken, E. R.; Gum, R. J.; Borhani, D. W.; Argiriadi, M.; Groebe, D. R.; Jia, Y.; Clampit, J. E.; Haasch, D. L.; Smith, H. T.; Wang, S.; Song, D.; Coen, M. L.; Cloutier, T. E.; Tang, H.; Cheng, X.; Quinn, C.; Liu, B.; Xin, Z.; Liu, G.; Fry, E. H.; Stoll, V.; Ng, T. I.; Banach, D.; Marcotte, D.; Burns, D. J.; Calderwood, D. J.; Hajduk, P. J. Discovery and characterization of non-ATP site inhibitors of the mitogen activated protein (MAP) kinases. *ACS Chem. Biol.* **2011**, *6* (3), 234−244.

(19) Voigt, J. H.; Bienfait, B.; Wang, S.; Nicklaus, M. C. Comparison of the NCI open database with seven large chemical structural databases. *J. Chem. Inf. Comput. Sci.* **2001**, *41* (3), 702−712.

(20) Fogolari, F.; Brigo, A.; Molinari, H. Protocol for MM/PBSA molecular dynamics simulations of proteins. *Biophys. J.* **2003**, *85* (1), 159−166.

(21) Halgren, T. A.; Nachbar, R. B. Merck molecular force field. IV. conformational energies and geometries for MMFF94. *J. Comput. Chem.* **1996**, *17* (5−6), 587−615.

(22) Middelbeek, J.; Clark, K.; Venselaar, H.; Huynen, M. A.; van Leeuwen, F. N. The alpha-kinase family: An exceptional branch on the protein kinase tree. *Cell. Mol. Life Sci.: CMLS* **2010**, *67* (6), 875−890.

(23) Soares, K. M.; Blackmon, N.; Shun, T. Y.; Shinde, S. N.; Takyi, H. K.; Wipf, P.; Lazo, J. S.; Johnston, P. A. Profiling the NIH Small Molecule Repository for compounds that generate H2O2 by redox cycling in reducing environments. *Assay Drug Dev. Technol.* **2010**, *8* (2), 152−174.

(24) Repici, M.; Mare, L.; Colombo, A.; Ploia, C.; Sclip, A.; Bonny, C.; Nicod, P.; Salmona, M.; Borsello, T. c-Jun N-terminal kinase binding domain-dependent phosphorylation of mitogen-activated protein kinase kinase 4 and mitogen-activated protein kinase kinase 7 and balancing cross-talk between c-Jun N-terminal kinase and extracellular signal-regulated kinase pathways in cortical neurons. *Neuroscience* **2009**, *159* (1), 94−103.